International Journal of Nanomedicine

Dovepress
open access to scientific and medical research

Open Access Full Text Article

ORIGINAL RESEARCH

CD44+/CD24− breast cancer cells exhibit phenotypic reversion in three-dimensional self-assembling peptide RADA16 nanofiber scaffold

This article was published in the following Dove Press journal:
International Journal of Nanomedicine
20 April 2015
Number of times this article has been viewed

Kun Mi[1]
Zhihua Xing[2]

[1]Department of Biochemistry and Molecular Biology, Sichuan Cancer Hospital and Institute, [2]Laboratory of Ethnopharmacology, Institute for Nanobiomedical Technology and Membrane Biology, West China Hospital, Sichuan University, Chengdu, People's Republic of China

Background: Self-assembling peptide nanofiber scaffolds have been shown to be a permissive biological material for tissue repair, cell proliferation, differentiation, etc. Recently, a subpopulation ($CD44^+/CD24^-$) of breast cancer cells has been reported to have stem/progenitor cell properties. The aim of this study was to investigate whether this subpopulation of cancer cells have different phenotypes in self-assembling $COCH_3$-RADARADARADARADA-$CONH_2$ (RADA16) peptide nanofiber scaffold compared with Matrigel® (BD Biosciences, Two Oak Park, Bedford, MA, USA) and collagen I.

Methods: CD44 and CD24 expression was determined by flow cytometry. Cell proliferation was measured by 5-bromo-2′-deoxyuridine assay and DNA content measurement. Immunostaining was used to indicate the morphologies of cells in three-dimensional (3D) cultures of different scaffolds and the localization of β-catenin in the colonies. Western blot was used to determine the expression of signaling proteins. In vitro migration assay and inoculation into nude mice were used to evaluate invasion and tumorigenesis in vivo.

Results: The breast cancer cell line MDA-MB-435S contained a high percentage (>99%) of $CD44^+/CD24^-$ cells, which exhibited phenotypic reversion in 3D RADA16 nanofiber scaffold compared with collagen I and Matrigel. The newly formed reverted acini-like colonies reassembled a basement membrane and reorganized their cytoskeletons. At the same time, cells cultured and embedded in RADA16 peptide scaffold exhibited growth arrest. Also, they exhibited different migration potential, which links their migration ability with their cellular morphology. Consistent with studies in vitro, the in vivo tumor formation assay further supported of the functional changes caused by the reversion in 3D RADA16 culture. Expression levels of intercellular surface adhesion molecule-1 were upregulated in cells cultured in RADA16 scaffolds, and the NF-kappa B inhibitor pyrrolidine dithiocarbamate could inhibit RADA16-induced upregulation of intercellular surface adhesion molecule-1 and the phenotype reversion of MDA-MB-453S cells.

Conclusion: Culturing a $CD44^+/CD24^-$-enriched breast cancer cell population in 3D RADA16 peptide nanofiber scaffold led to a significant phenotypic reversion compared with Matrigel and collagen I.

Keywords: 3D culture, phenotype, reversion

Introduction

Tumors are being increasingly perceived as hierarchically organized heterogeneous populations of cells with a small fraction of tumor cell compartment which is capable of initiating a new tumor. Because of the features that these cells share with somatic stem cells, they have been termed cancer stem cells (CSCs).[1,2] It has been long acknowledged that microenvironment plays a role as regulator of tumor progression. Tumor cells communicate with their surrounding microenvironment, receiving molecular cues

Correspondence: Kun Mi
Department of Biochemistry and Molecular Biology, Sichuan Cancer Hospital and Institute, No 55, Section 4, South People's Road, Chengdu 610041, Sichuan, People's Republic of China
Tel +86 28 8542 0256
Fax +86 28 8542 0116
Email mikun@126.com

that direct diverse cellular phenotypes.[3–5] Stem cells reside in a stem cell microenvironment that regulates the fate of the stem cell with respect to self-renewal, quiescence, and differentiation.[6] Although the role of niche microenvironments in the biology of CSCs has just started to be explored,[7–13] it is reasonable to suggest that the plasticity between the differentiation states of cancer cells and the regulation by microenvironmental cues provide new starting-points for novel cancer therapies.

Three-dimensional (3D) culture of cancer cells has been used as an important model to provide invaluable insight into cancer biology and most closely mimic tumorigenicity in vivo.[14,15] Previously, most cell culture experiments have been performed under adherent two-dimensional (2D) conditions, which could not truly reflect the complex interactions between cancer cells and the microenvironment that plays a critical role in controlling cell behavior, tumor development and progression. Conventional 2D cancer cell culture has proven to be limited in modeling some of the critical aspects of cell biology, such as 3D microenvironment, 3D gradient diffusion, and 3D cell–cell contact interactions. Researchers have shown recently that there are important differences in the behavior of cancer cells grown in 2D and 3D cultures.[16–21] 3D scaffolds can provide important physical and biochemical influence to various receptors. Meanwhile, the gelatinous scaffolds can provide more pliable microenvironments than tissue culture plastic and better mimic the microenvironments in vivo. The design, fabrication, and application of nanomaterials such as self-assembly peptides[22–24] and electrospun nanofibers[25–27] have provided an advantageous model for nanotechnology scientists in their use for tissue engineering and biomedical research.

Breast cancer stem cells (BCSCs) constitute a subpopulation of tumor cells that express stem cell-associated makers and have a high capacity for tumor generation in vivo. Identification of BCSCs from tumor samples or breast cancer cell lines has been based mainly on $CD44^+/CD24^-$ or aldehyde dehydrogenase markers.[28–30] Taking advantage of the $CD44^+/CD24^-$-enriched cell population that mostly comprises the MDA-MB-435S mesenchymal cancer cell line, we provide evidence that $CD44^+/CD24^-$ breast cancer cells exhibit partial phenotypic reversion in 3D self-assembling peptide $COCH_3$-RADARADARADARADA-$CONH_2$ (RADA16) nanofiber scaffold compared with collagen I and Matrigel® (BD Biosciences, Two Oak Park, Bedford, MA, USA) scaffolds.

The aim of this study was to investigate whether this subpopulation of cancer cells has different phenotypes in different 3D scaffolds and to examine whether that microenvironment is important not only for the survival but also for the maintenance of the undifferentiated state of BCSCs. This is the first report of the putative extracellular matrix microenvironment revert of the $CD44^+/CD24^-$ cancer cell subpopulation phenotype in breast cancer by 3D culture.

Materials and methods

Cell culture

The MDA-MB-435S cell line was obtained from the American Type Culture Collection (Manassas, VA, USA). The cell line was cultured in L-15 medium supplemented with insulin (0.01 mg/mL) and 10% fetal bovine serum (FBS). RADA16 solution (1%) was purchased as PuraMatrix (BD Bioscience, San Jose, CA, USA) and was dissolved in water at a final concentration of 1% (weight/volume) and sonicated for 20 minutes. Rat-tail collagen I and growth factor-reduced Matrigel matrix were purchased from BD Biosciences. For 3D cultures, cells cultured on plastic were trypsinized, washed, and pelleted by centrifugation. For Matrigel cultures, cells were plated in a 1:1 dilution of Matrigel at 5×10^5 cells/mL and overlaid with culture medium. Collagen I gels were prepared according to the manufacturer's instructions, with a final concentration of 1.5 mg/mL. Experiments were carried out in 24-well dishes using collagen I and single cell suspensions. Whenever coculture experiments were performed, the interacting cells were premixed in equal numbers in suspension prior to embedding in gels. After 30 minutes incubation at 37°C, the gelled block of cells were overlaid with the culture medium. This medium was subsequently changed at 2-day intervals. For RADA16 peptide, a mixture of 1% RADA16 and cell suspension in sucrose solution was poured at a volume of 50 μL/well, followed by the slow addition of basal medium. The contents were allowed to self-assemble for 20 minutes and were rinsed once with culture medium to wash away any acid residue remaining from peptide synthesis. The media were changed every 2 days.

Flow cytometry

Cells were washed once with phosphate-buffered saline (PBS) and then harvested with 0.05% trypsin/0.025% EDTA. Detached cells were washed with PBS containing 1% FBS and 1% penicillin/streptomycin (wash buffer) and resuspended in the wash buffer at a concentration of 10^6 cells in 100 μL. Combinations of fluorochrome-conjugated monoclonal antibodies obtained from BD Biosciences against human CD44 (fluorescein isothiocyanate; catalog #555478) and CD24 (phycoerythrin; catalog #555428) or their respective isotype controls were added to the cell suspension

at concentrations recommended by the manufacturer and incubated at 4°C in the dark for 30–40 minutes. Cells were washed in the wash buffer, resuspended in PBS, and analyzed on a Canto II flow cytometer (BD Biosciences).

Structural study using atomic force microscopy

After stationary incubation at 4°C overnight, 5 µL samples of the working solutions of Matrigel, collagen I, and RADA16 were immediately deposited onto a freshly cleaved mica surface and left for 15 seconds, then rinsed with distilled water to remove unattached materials. The sample was then air-dried. Atomic force microscopy (AFM) images were collected with a SPI4000 Probe Station and SPA-400 SPM Unit (Seiko Instruments Inc., Chiba, Japan) with a resonance frequency of 120 kHz, spring constant 12 N/m, tip curvature radius 10 nm, and 200 µm length. AFM images were obtained in tapping mode. Typical scanning parameters were as follows: tapping frequency 120 KHz, root mean square (RMS) amplitude before engage ~1.0 V, integral and proportional gains of 0.1–0.6 and 0.05–0.2, respectively, and scan rate 1.0 Hz.

Immunostaining

3D cultures were washed with PBS and fixed with 4% paraformaldehyde for 15 minutes at room temperature, then washed with PBS three times. For immunostaining, cultures were blocked with 10% goat serum (v/v) in immunofluorescence buffer (0.2% Triton X-100, 0.1% bovine serum albumin, 0.05% Tween 20 in PBS [pH 7.4; sterilized by 0.22 µm filter]).[31] The 4′,6-diamidino-2-phenylindole, dihydrochloride (DAPI), rhodamine phalloidin, and calcein AM were puchased from MolecularProbes (Thermo Fisher Scientific, Waltham, MA, USA). For viability studies, a working solution containing 2 µM calcein AM was prepared according to the manufacturer's instructions, and 200 µL of this stock was added to each well. For morphology immunostaining, working solution of rhodamine phalloidin (5 U/mL) and DAPI (300 nM) were diluted in PBS buffer for F-actin and nuclear staining, respectively. Immunofluorescent images were obtained with an Olympus X 71 inverted microscope (Olympus Corporation, Tokyo, Japan).

Cell proliferation analysis

3D cultures were prepared with the following exceptions: 10 mM 5-bromo-2′-deoxyuridine (BrdU) was added to the culture medium 12 hours prior to the culture without fixative. Cultures were fixed in 4% paraformaldehyde in PBS for 15 minutes, followed by a 30-minute incubation in 2 M HCl, all performed at room temperature. Staining proceeded using anti-BrdU 1:100 and goat anti-mouse immunoglobulin-fluorescein isothiocyanate 1:100. BrdU-labeled nuclei were scored with 200 cells per experiment, and indexes were expressed by the percentage of labeled number in the total nuclei.

DNA content measurement

The number of cells in the scaffold was determined by the fluorometric quantification of amount of cellular DNA. The cell-seeded scaffold was rinsed with PBS and recovered by Na citrate buffer solution containing 50 mM Na citrate and 100 mM NaCl and stored at −80°C until assay. After thawing, the cells were lysed in the Na citrate solution with occasional mixing. The 10 µL of cell lysate was mixed with fluorescent assay buffer and DNA-binding fluorescent dye solution (Hoechst 33258). The fluorescence intensity of the mixed solution was measured on a fluorescence spectrometer (Hitachi F-7000; Hitachi Ltd., Tokyo, Japan) at excitation 360 nm/emission 460 nm. The calibration curve between the DNA and cell number was prepared by use of cell suspensions with different cell densities.

In vitro migration analysis

Cells were serum-deprived for 24 hours, then 2.5×10^4 cells were seeded as 3D cultures according to the methods mentioned previously in triplicate on fibronectin-coated inserts, moved to chambers containing 350 µL of 10% FBS as a chemoattractant, and incubated for 24 hours. After 24 hours in culture, cells were fixed with methanol and stained with 0.5% toluidine blue in 2% Na_2CO_3. Cells on the upper side of the chamber were removed, and cells on the lower chamber were visualized and counted. Each experiment was repeated three times in duplicate.

Western blot

Proteins were extracted from cells using RIPA buffer (10 mM Tris-HCl [pH 7.4], 10 mM EDTA-Na_2, 0.8% [weight/volume] NaCl, 10 mM iodoracetamide, 1% [wt/v] deoxycholate, 0.1% [wt/v] sodium dodecyl sulfate (SDS), and protease inhibitor cocktail), and insoluble material was removed by centrifugation at 22,000 g for 30 minutes. Protein electrophoresis was performed by standard SDS-PAGE methods, using reducing sample buffer. Proteins were transferred to polyvinylidene fluoride membranes and blocked in 5% nonfat dried milk in TBST buffer (10 mM Tris-HCl [pH 7.4], 100 mM NaCl, 0.05% [v/v] Tween 20). All of the antibodies were diluted in the blocking buffer. Membranes were washed in TBST

buffer. Antibody binding was detected using secondary antibodies and the SuperSignal chemiluminescent substrate (Thermo Fisher Scientific), according to the manufacturer's instructions.

Tumorigenesis in vivo

MDA-MB-435S cells were propagated as monolayers, trypsinized, washed three times in L-15 medium, pelleted by centrifugation, resuspended in L-15 medium, and mixed with different scaffolds following standard cell culture procedures. 1×10^7 cells were immediately injected subcutaneously into the mammary fat pads of 4–6-week-old BALB/c nude mice in the form of suspension mixtures of cells and scaffolds. 2D cells were injected into nude mice as control. L-15 medium without cells and scaffolds without cells were also injected into nude mice as negative controls.

Ethics statement

Care of laboratory animals and experimentation on animals were in accordance with animal ethics guidelines and approved protocols. All animal studies were approved by the Institutional Ethics Committee of Sichuan University.

Results

Prospective stem cell markers were differentially expressed in human breast cancer cell lines

Flow cytometry was used to assess the expression of prospective CSC markers of CD44/CD24. We investigated three human breast cancer cell lines, MDA-MB-231, MDA-MB-435S, BT-549, and one normal breast cell line MCF 10A as normal cell line control. The results indicated that the breast cancer cell line MDA-MB-435S had the highest proportion of $CD44^+/CD24^-$ cells (99.4%), whereas BT549 had the lowest proportion of $CD44^+/CD24^-$ cells (0.8%) (Figure 1). Taking advantage of the $CD44^+/CD24^-$-enriched cell population that mostly comprises the MDA-MB-435S mesenchymal cancer cell line, we could then analyze their phenotypes in different 3D scaffolds of collagen I, Matrigel, and the self-assembling peptide RADA16.

The morphologies of breast cancer cell line MDA-MB-435S in 3D cultures of different scaffolds

AFM results showed that the nanofibers formed by self-assembly of RADA16 peptides have similar nanoscale with animal-derived Matrigel and collagen I nanostructures and could mimic the 3D microenvironment in vivo by using extracellular matrix substitutes (Figure 2A). MDA-MB-435S cells exhibit various 3D morphologies in response to different 3D culture scaffolds, which were identified by light microscopy and localization of F-actin in colonies at the endpoint of 5 days (Figure 2B and C). In this study, cells grown in collagen I showed elongated cell bodies with projections and disorganized nuclei, indicating a spindle-shaped mesenchymal phenotype and implying their invasive potential. Cells in Matrigel form colonies with nuclei that are disorganized, showing an apolar, disorganized phenotype while the colonies in RADA16 form round colonies and nuclei organized in a regular pattern around the center. They also have robust cell–cell adhesion, indicated by fluorescence microscopy, which resembles the nonmalignant phenotype of mammary cells. The cells in RADA16 cultures can be somewhat "reverted" to a phenotype much more approximating that of nonmalignant breast acini (Figure 2C). They reorganized their cytoskeletons and showed basally-localized nuclei and organized filamentous F-actin. MDA-MB-435S cell distribution and viability was examined in the different scaffolds using calcein-AM staining, which stains whole living cells (Figure 2D).

The proliferation and migration potential of MDA-MB-435S in different scaffolds

Cells cultured in RADA16 peptide, Matrigel, and collagen I scaffolds were evaluated for viable cell density by using the DNA content assay (Figure 3A). In Matrigel and collagen I scaffolds, cell density continued to increase between day 3 and 9 while in RADA16, cell density increased actively before day 5 and increased slowly between day 5 and 7, indicating a growth arrest, until cells then decreased between day 7 and 9, as some began to die. BrdU incorporation in these scaffolds further delineated DNA content results (Figure 3B). More than 90% of cells in RADA16 were growth-arrested as compared with cells grown in other scaffolds that continued to synthesize DNA after day 5. The migration behavior of cells was analyzed as a demonstration of metastasis potential and was quantified by Boyden chamber assay, with some modification. Four and a half percent of cells cultured in RADA16 and 29% of cells cultured in Matrigel migrated through the matrix on the 8 μm membranes compared to almost all cells cultured in collagen I, which migrated through (Figure 3C). The migration capability of tumor cells was strongest in collagen I, which showed an invasive phenotype, and weakest in RADA16, indicative of connections between spheroid formation and invasion capabilities. The results reflect the fact that cells have less metastasis potential when in the form of spheroids as opposed to elongated

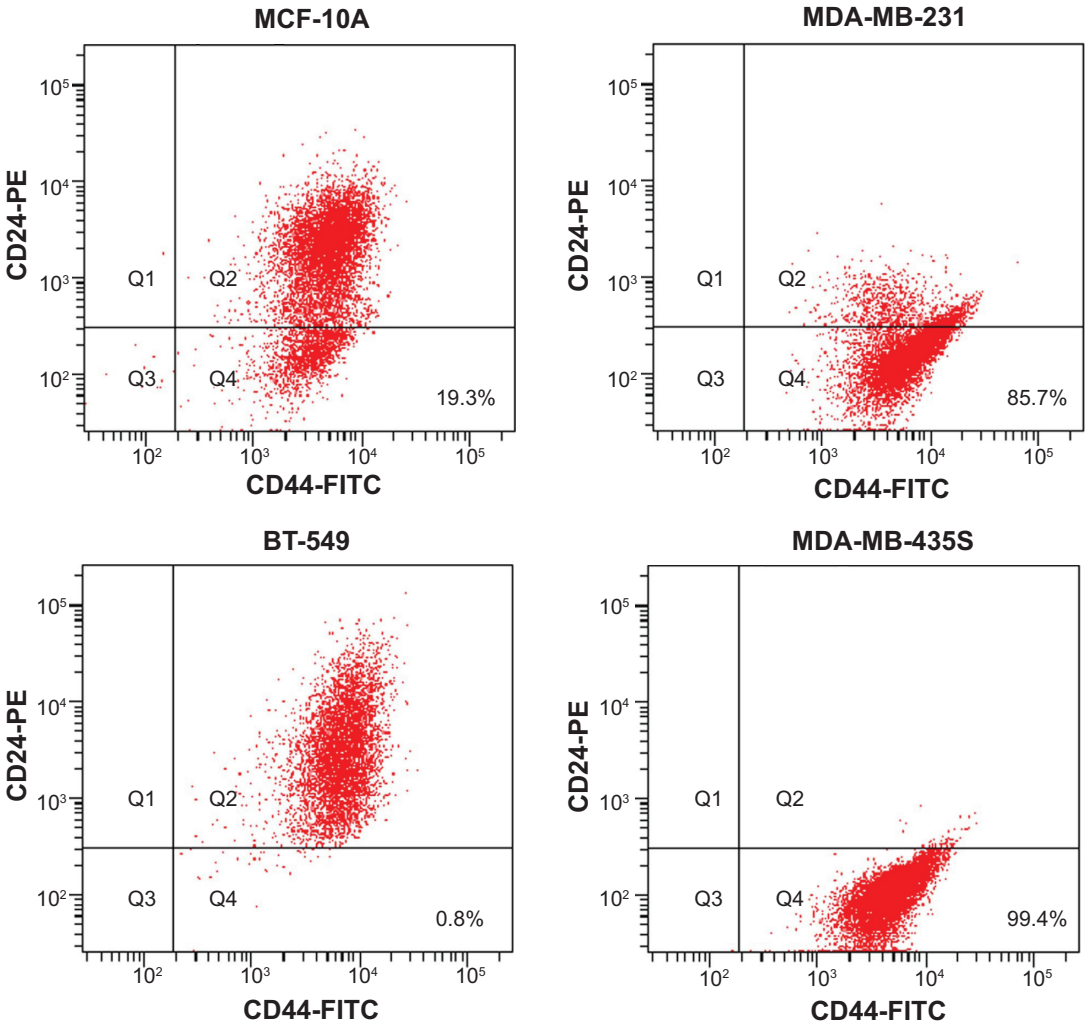

Figure 1 Identification of a $CD44^+/CD24^-$ subpopulation in breast cancer cell lines MCF-10A, MDA-MB-231, BT-549, and MDA-MB-435S by flow cytometry.
Notes: Cells in Q4 correspond to $CD44^+/CD24^-$ cells. MDA-MB-435S shows highest proportion of $CD44^+/CD24^-$ antigen phenotype among other cell lines.
Abbreviations: FITC, fluorescein isothiocyanate; PE, phycoerythrin.

cells in the mesenchymal form. Also, the large, loose aggregates in Matrigel, having poor cell–cell adhesion, were more invasive than the spheroids in RADA16, having robust cell–cell adhesion, which restricted cancer cell migration.

The localization and expression of signaling proteins in RADA16 cells colonies

Hematoxylin staining of cryostat sections of the scaffolds confirmed lumen formation in RADA16 only, not in Matrigel (Figure 4A). The nuclei of cell colonies stained with DAPI also showed lumen formation in RADA16 and irregular organization in Matrigel (Figure 4B). Immunofluorescence revealed the localization of β-catenin in the colonies of RADA16 (Figure 4C). Acini-like structures established tissue polarity in RADA16 as shown by β-catenin at cell–cell junctions. They revealed uniform and polarized nuclei, well-organized filamentous actin, and β-catenin at the lateral cell–cell junctions. In contrast, cells cultured in 3D Matrigel had polymorphic nuclei and a grossly disorganized actin cytoskeleton (Figure 4C). Western blot analysis showed that there were consistently high expression levels of β-catenin since day 6 in RADA16 culture. The expression of β-catenin was highest in RADA16 culture, lower in collagen I culture, and lowest in Matrigel culture. On day 9, the expression of β-catenin in cells in collagen I declined while there were no significant changes in RADA16 (Figure 4D). To some extent, these data correspond with results of studies conducted by Weaver et al and Wang et al who investigated the reversion of breast cancer cells.[16,18] They, however, conducted the reversion by using certain antibodies in 3D Matrigel culture instead of the self-assembling

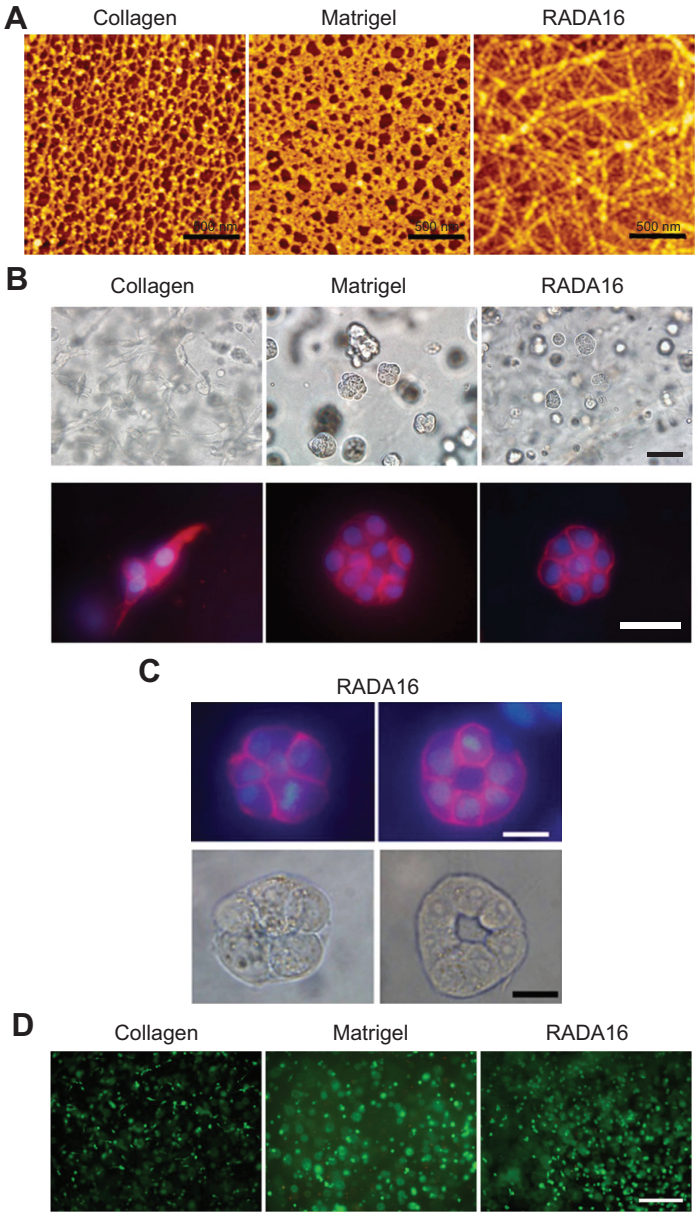

Figure 2 The reversion of the malignant phenotype in the morphology of breast cancer cell line MDA-MB-435S in RADA16 compared with Matrigel® and collagen I scaffolds.

Notes: (**A**) AFM images of collagen I, Matrigel, and RADA16 peptide nanofiber scaffolds. Scale bars represent 500 nm. (**B**) Light microscope images (upper) and F-actin and nuclear fluorescence images (lower) of cells encapsulated in collagen I, Matrigel, and RADA16 peptide scaffolds. Three-dimensional cultures were stained for F-actin, and nuclei were counterstained with DAPI. Scale bars represent 100 μm (upper) and 50 μm (lower). (**C**) F-actin and nuclear fluorescence images (upper) and light microscope images (lower) of most common morphology of polarized cell colonies formed in RADA16 scaffold. Scale bars represent 25 μm. (**D**) Encapsulation of cells in different scaffolds using calcein-AM staining for the living cells. Scale bar represents 500 μm. Matrigel® (BD Biosciences, Two Oak Park, Bedford, MA, USA).

Abbreviations: AFM, atomic force microscopy; DAPI, 4′,6-diamidino-2-phenylindole, dihydrochloride; RADA16, $COCH_3$-RADARADARADARADA-$CONH_2$.

peptide nanofiber scaffold. Intercellular surface adhesion molecule-1 (ICAM-1), the protein involved in NF-kappa B (NF-κB) signaling processes and in cell–cell and cell–extracellular matrix interactions, was also analyzed by Western blot (Figure 4D). ICAM-1 expression was significantly upregulated in cells in RADA16 culture compared to cells in the collagen I and Matrigel groups. During the culture process, the expression of ICAM-1 in the Matrigel group remained at low levels but declined from day 6 in the collagen I group. The expression of ICAM-1 was highest in cells in the RADA16 group, indicative of the active role of ICAM-1 in cellular interactions.

Culture in RADA16 peptide nanofiber scaffold resulted in loss of malignancy in vivo

To determine the relationship between phenotypic reversion of tumor cells and tumorigenicity in vivo, we injected tumor

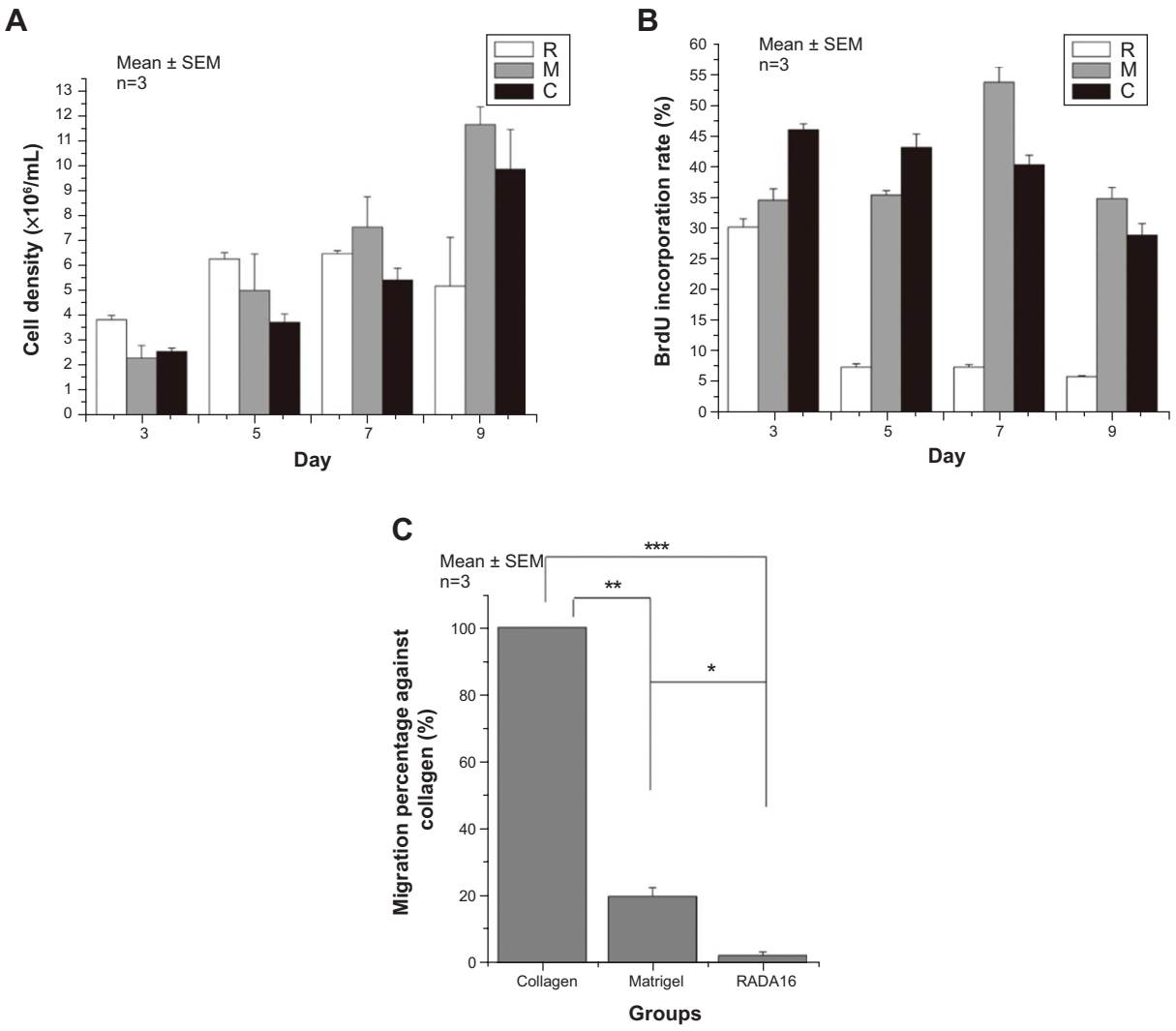

Figure 3 The reversion of the malignant phenotype in the proliferation and migration potential of breast cancer cell line MDA-MB-435S in RADA16 compared with Matrigel® and collagen I scaffolds.

Notes: (**A**) Cell density in different scaffolds calculated from DNA measurement after 3-day, 5-day, 7-day, and 9-day culture. (**B**) Percentage of BrdU labeling in cells grown in different scaffolds expressed as the BrdU labeling index from three separate experiments (about 200 cells/experiment) on days 3, 5, 7, and 9. (**C**) Migration potential of MDA-MB-435S cells in Matrigel, collagen I, and RADA16 scaffolds; *$P<0.05$; **$P<0.001$; ***$P<0.0001$. Matrigel® (BD Biosciences, Two Oak Park, Bedford, MA, USA).

Abbreviations: BrdU, 5-bromo-2′-deoxyuridine; C, collagen; M, Matrigel; R, RADA16; SEM, standard error of the mean; RADA16, $COCH_3$-RADARADARADARADA-$CONH_2$.

cells after culturing them in 3D scaffolds into nude mice. Tumor growth was observed in mice injected with cells previously cultured in Matrigel and collagen I but not with those cultured in RADA16. After sacrificing the mice, we observed no tumor formation in the RADA16 group, in which the malignant potential in vivo is lost. These data suggested that the tumor cell phenotype in 3D culture directly affects the malignancy in vivo (Figure 5).

Blocking NF-κB signaling inhibited the reversion phenotype of MDA-MB-435S cells via the downregulation of ICAM-1

To gain further insight into the mechanism involved in the reversion phenotype induced by RADA16 3D culturing of MDA-MB-435S cells, we first examined the potential involvement of NF-κB signaling in the regulation of ICAM-1 expression. By using the NF-κB inhibitor pyrrolidine dithiocarbamate (PDTC) we demonstrated that it significantly inhibited RADA16-induced upregulation of ICAM-1 in MDA-MB-435S cells (Figure 6A). Next, we examined the effects of PDTC on the reversion phenotype and found that the phenotype changes of MDA-MB-453S cells induced by RADA16 3D culturing were prevented by PDTC (Figure 6B). Cell colonies showed a disorganized, apolar phenotype, which resembled cells in Matrigel. These results suggest that 3D culturing in RADA16 nanofiber scaffold leads to the activation of NF-κB signaling in MDA-MB-435S cells, which in turn upregulates ICAM-1 expression and induces the reversion of MDA-MB-435S cells.

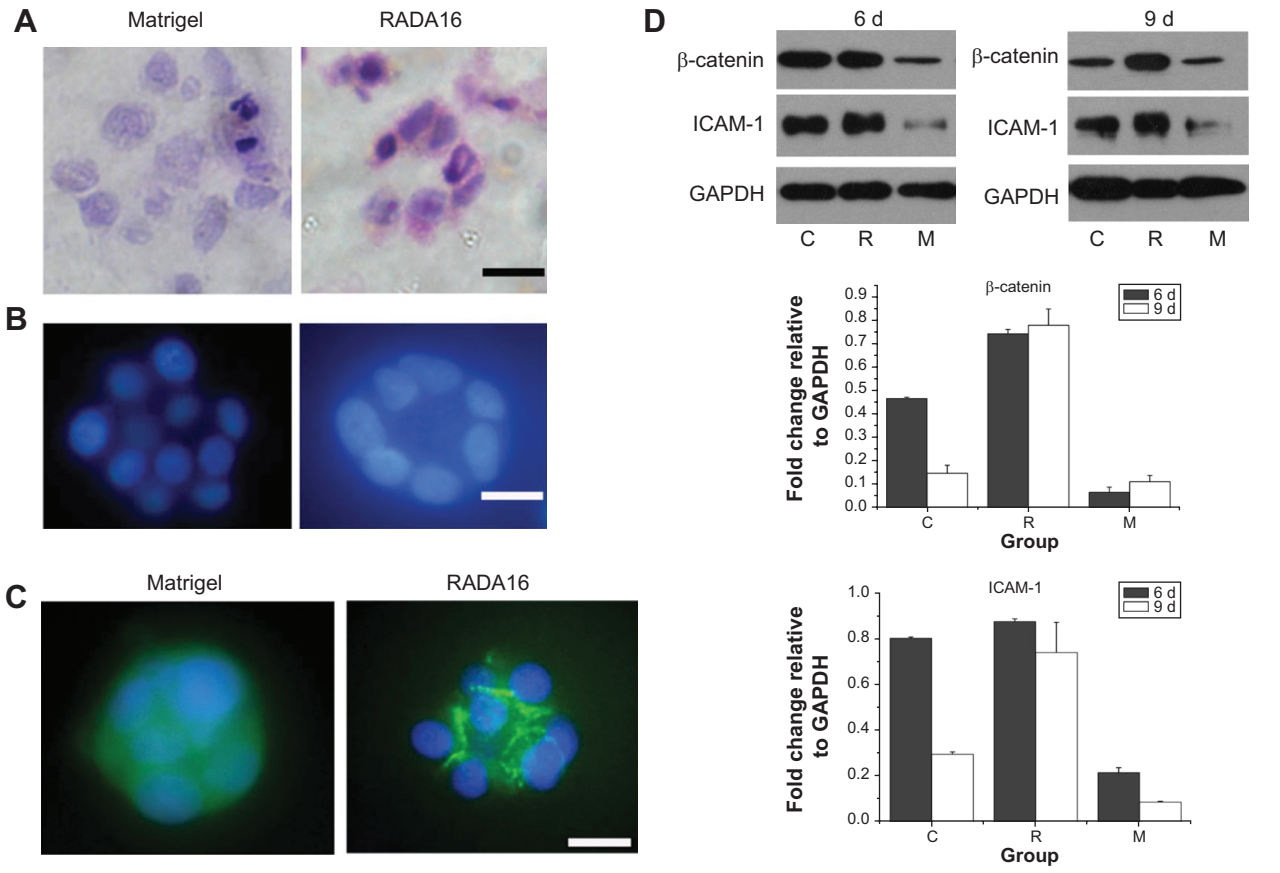

Figure 4 Cellular characteristics and the localization and expression of signaling proteins in RADA16 cells colonies.

Notes: (**A**) Hematoxylin staining of cryostat sections of the Matrigel and RADA16 scaffolds show lumen formation only in RADA16 scaffold. Scale bar represents 25 μm. (**B**) The nuclei of cell colonies stained with DAPI show lumen formation in RADA16 and irregular organization in Matrigel. Scale bar represents 25 μm. (**C**) Immunolocalization of β-catenin (green) with DAPI stained nuclei (blue) in RADA16 and Matrigel scaffolds. The β-catenin is diffusely localized in the cytoplasm, nucleus, and some cell–cell contacts within colonies formed in Matrigel but forms intense localization in the cell–cell junctions in colonies formed in RADA16, indicating similar β-catenin distribution like that of nonmalignant S-1 cells.[32] Scale bar represents 25 μm. (**D**) Western blot analysis of the indicated proteins β-catenin and ICAM-1 of MDA-MB-435S cells in different three-dimensional cultures at 6 days and 9 days. Equal amounts of protein were loaded per lane, and GAPDH was run as a control for equal loading and exposure time. Matrigel® (BD Biosciences, Two Oak Park, Bedford, MA, USA).

Abbreviations: 6 d, 6-day cultures; 9 d, 9-day cultures; C, collagen; DAPI, 4′,6-diamidino-2-phenylindole, dihydrochloride; GAPDH, glyceraldehyde-3-phosphate dehydrogenase; ICAM-1, intercellular surface adhesion molecule-1; M, Matrigel; R, RADA16; RADA16, $COCH_3$-RADARADARADARADA-$CONH_2$.

Discussion

To identify whether the reversion was reversible and whether the phenomenon was caused by the effect of microenvironment or genetically changed mutants, we carried out a series of reversion and recovery studies. Despite two rounds of reversion in 3D RADA16 scaffold, recovery in 2D for monolayer propagation, and regrowth in 3D RADA16 scaffold, these cells were able to maintain their original phenotype when cultured in the 2D monolayer. We can see then, the reversion is phenotypic and reversible. These data suggest a phenotypic plasticity model in which phenotypic heterogeneity is driven largely by reversible changes directed by the microenvironment rather than by irreversible genetic changes. Our previous work has indicated that the RADA16 self-assembling peptide scaffold could effectively reduce the malignant phenotype of breast cancer cells.[33] Research by Ling et al has suggested that self-assembling peptide can inhibit the formation of metastatic prostate CSC colonies in vitro, while preserving its viability and CSC property.[34]

Our results show that the $CD44^+/CD24^-$ cell population-enriched breast cancer cell line adopts various morphologies in different 3D culture scaffolds in response to cues from the extracellular matrix. In this assay, the disorganized malignant phenotype of the cells can partially be reverted to a phenotype much more closely approximating that of nonmalignant breast acini in RADA16 3D cultures. In the first 5 days, the colonies in RADA16 and Matrigel were similar in size and roundness. Roundness is defined as

$$P^2/(4\pi A) \quad (1)$$

where P is the perimeter and A is the area of the colonies. It is a perfect circle when this value is equal to 1. A value

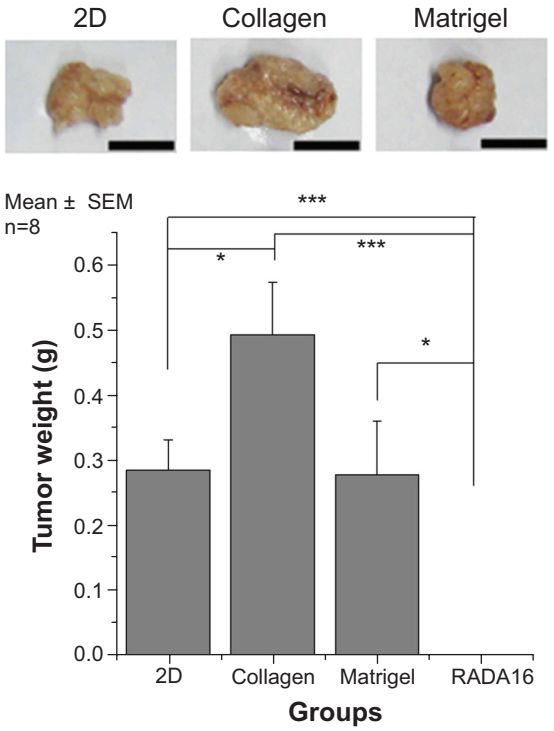

Figure 5 Effect of phenotype reversion of cells in RADA16 on tumorigenicity in vivo compared to collagen I and Matrigel.

Notes: 2D cells were injected into nude mice as control. Scale bars represent 1 cm. Cells with a reversion in phenotype resulted in the loss of tumorigenicity in the nude mice; $^{*}P<0.05$; $^{***}P<0.0001$. Matrigel® (BD Biosciences, Two Oak Park, Bedford, MA, USA).

Abbreviations: 2D, two-dimensional group; SEM, standard error of the mean; RADA16, $COCH_3$-RADARADARADARADA-$CONH_2$.

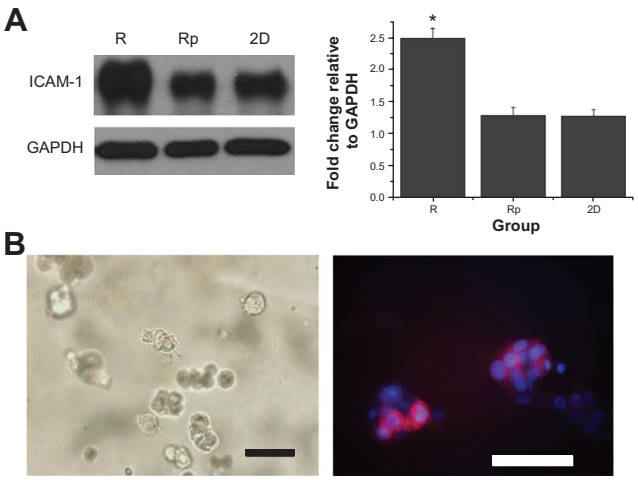

Figure 6 The reversion phenotype of MDA-MB-435S cells was inhibited by blocking NF-κB signaling by PDTC.

Notes: (**A**) Western blot analysis of ICAM-1 of MDA-MB-435S cells in different culture groups. Equal amounts of protein were loaded per lane, and GAPDH was run as a control for equal loading and exposure time. The expression of ICAM-1 of cells in RADA16 was significantly downregulated by PDTC ($^{*}P<0.05$). (**B**) Light microscope images and F-actin and nuclear fluorescence images of cells in PDTC-treated RADA16 group. Three-dimensional cultures were stained for F-actin, and nuclei were counterstained with DAPI. Scale bars represent 100 μm (left) and 50 μm (right).

Abbreviations: 2D, two dimensional group; DAPI, 4′,6-diamidino-2-phenylindole, dihydrochloride; GAPDH, glyceraldehyde-3-phosphate dehydrogenase; ICAM-1, intercellular surface adhesion molecule-1; PDTC, pyrrolidine dithiocarbamate; R, RADA16 group; Rp, RADA16 + PDTC group; RADA16, $COCH_3$-RADARADAR-ADARADA-$CONH_2$.

of >1 demonstrates the amount of deformation compared to a circle.[35] After 5 days, colonies in Matrigel actively grow, both in size and morphology, showing large, loose, and irregular shapes, with increasing roundness values from 2 to 18. However, colonies in RADA16 maintained a much smaller spheroid shape with roundness values between 1.3 and 1.7. By applying the morphogenesis criteria suggested by Weaver et al[16] we studied the reversion rate of $CD44^+/CD24^-$ cells in 3D RADA16, which was 73.55%±1.454% on day 7, suggesting the phenotype was partially reverted. Meanwhile, the on-top culture model results indicated no phenotype reversion, which implied that only the 3D-embedding culture model in RADA16 scaffold could lead to the reversion.

Sheridan et al have reported that the $CD44^+/CD24^-$ phenotype of breast cancer cells is associated with invasive properties.[36] Our results indicate the invasive potential of $CD44^+/CD24^-$ breast cancer cells was dramatically reduced by RADA16 3D culture, suggesting that extracellular matrix plays an important role in metastasis and tumorigenesis of $CD44^+/CD24^-$ breast cancer cells. The data support that even malignant CSC cells are plastic and dependent on microenvironmental signals for their survival, differentiation, and metastasis.

Li et al have pointed out that there was a direct relationship between upregulation of ICAM-1 and NF-κB signaling.[37] ICAM-1 is constitutively expressed at low levels on the surface of a wide variety of cells, including fibroblasts, leukocytes, keratinocytes, endothelial cells, hepatocytes, smooth muscle, and epithelial cells.[38] ICAM-1 has five immunoglobulin-like domains, which function in mediating cell–cell and cell–extracellular matrix interactions. To gain further insight into the mechanisms involved in RADA16-induced phenotypic reversion, we performed Western blot experiments and revealed the engagement of ICAM-1 and NF-κB signaling in this process. Blockade of this signaling pathway in RADA16-cultured cells may inhibit ICAM-1 expression and reversion of phenotype.

Although we identified changes of expression and localization of some important signaling proteins, further investigation is still needed to fully understand the reversion mechanism. It is likely that the MDA-MB-435S cells, mostly composed of a $CD44^+/CD24^-$ cell population, have the ability to redifferentiate in this scaffold, which excludes some exogenously-exerting influences such as growth factors and matrix proteins in Matrigel and collagen I.

It is necessary to mention that the origin of the MDA-MB-435S cell is questionable; some researchers suggested it may have evolved from a melanoma cell line[39,40] while more recently, MDA-MB-435S cells have been described as

breast cancer cells that express melanocytic differentiation markers.[41] By using the peptide RADA16 scaffold, rather than genetic means, we have achieved phenotype reversion in a particular cell population with $CD44^+/CD24^-$ antigen. This provides a new perspective in cancer research and therapy whereby we can target the cell culture microenvironment. As a result, the stem cell niche has become a novel target of cancer therapeutics. Self-assembling peptide may be an effective nanomaterial for inhibiting metastasis and cancer progression.

Conclusion

In this report, we show the different phenotypes of $CD44^+/CD24^-$ breast cancer cells in RADA16 peptide nanofiber scaffold, Matrigel, and collagen I. The $CD44^+/CD24^-$ phenotype is associated with stem/progenitor cell properties. Our surprising finding was the significant phenotypic reversion of $CD44^+/CD24^-$ breast cancer cells in 3D RADA16 peptide nanofiber scaffold, which resembles the nonmalignant phenotype of mammary cells. Our studies suggest that RADA16 induced the phenotypic reversion through NF-κB signaling-dependent upregulation of ICAM-1.

Acknowledgments

We thank Zijia Liu, Guixia Wang, Ben Huang, Yang Ye, Jianming Huang, Shiqi Ma for helpful discussions and assistance. This research was financially supported by the National Natural Science Foundation of China (Grant No 81201826). This work was partly supported by the China National 985 Project, and some tests were completed at Sichuan University.

Disclosure

The authors report no conflicts of interest in this work.

References

1. Nguyen LV, Vanner R, Dirks P, Eaves CJ. Cancer stem cells: an evolving concept. *Nat Rev Cancer*. 2012;12(2):133–143.
2. Kreso A, Dick JE. Evolution of the cancer stem cell model. *Cell Stem Cell*. 2014;14(3):275–291.
3. Park CC, Bissell MJ, Barcellos-Hoff MH. The influence of the microenvironment on the malignant phenotype. *Mol Med Today*. 2000; 6(8):324–329.
4. Radisky D, Muschler J, Bissell MJ. Order and disorder: the role of extracellular matrix in epithelial cancer. *Cancer Invest*. 2002;20(1):139–153.
5. Postovit LM, Seftor EA, Seftor RE, Hendrix MJ. Influence of the microenvironment on melanoma cell fate determination and phenotype. *Cancer Res*. 2006;66(16):7833–7836.
6. Tieu KS, Tieu RS, Martinez-Agosto JA, Sehl ME. Stem cell niche dynamics: from homeostasis to carcinogenesis. *Stem Cells Int*. 2012; 2012:367567.
7. Boral D, Nie D. Cancer stem cells and niche microenvironments. *Front Biosci (Elite Ed)*. 2012;4:2502–2514.
8. Zhu X, Zhou X, Lewis MT, Xia L, Wong S. Cancer stem cell, niche and EGFR decide tumor development and treatment response: A bio-computational simulation study. *J Theor Biol*. 2011;269(1):138–149.
9. Shiozawa Y, Pedersen EA, Havens AM, et al. Human prostate cancer metastases target the hematopoietic stem cell niche to establish footholds in mouse bone marrow. *J Clin Invest*. 2011;121(4):1298–1312.
10. Pasquier J, Rafii A. Role of the microenvironment in ovarian cancer stem cell maintenance. *Biomed Res Int*. 2013;2013:630782.
11. Sottoriva A, Sloot PM, Medema JP, Vermeulen L. Exploring cancer stem cell niche directed tumor growth. *Cell Cycle*. 2010;9(8): 1472–1479.
12. Chen L, Xiao Z, Meng Y, et al. The enhancement of cancer stem cell properties of MCF-7 cells in 3D collagen scaffolds for modeling of cancer and anti-cancer drugs. *Biomaterials*. 2012;33(5):1437–1444.
13. Zhu TS, Costello MA, Talsma CE, et al. Endothelial cells create a stem cell niche in glioblastoma by providing NOTCH ligands that nurture self-renewal of cancer stem-like cells. *Cancer Res*. 2011; 71(18):6061–6072.
14. Smalley KS, Lioni M, Herlyn M. Life isn't flat: taking cancer biology to the next dimension. *In Vitro Cell Dev Biol Anim*. 2006;42(8–9):242–247.
15. Kim JB. Three-dimensional tissue culture models in cancer biology. *Semin Cancer Biol*. 2005;15(5):365–377.
16. Weaver VM, Petersen OW, Wang F, et al. Reversion of the malignant phenotype of human breast cells in three-dimensional culture and in vivo by integrin blocking antibodies. *J Cell Biol*. 1997;137(1):231–245.
17. Wang F, Weaver VM, Petersen OW, et al. Reciprocal interactions between beta1-integrin and epidermal growth factor receptor in three-dimensional basement membrane breast cultures: a different perspective in epithelial biology. *Proc Natl Acad Sci U S A*. 1998;95(25): 14821–14826.
18. Wang F, Hansen RK, Radisky D, et al. Phenotypic reversion or death of cancer cells by altering signaling pathways in three-dimensional contexts. *J Natl Cancer Inst*. 2002;94(19):1494–1503.
19. Wolf K, Mazo I, Leung H, et al. Compensation mechanism in tumor cell migration: mesenchymal-amoeboid transition after blocking of pericellular proteolysis. *J Cell Biol*. 2003;160(2):267–277.
20. Anders M, Hansen R, Ding RX, Rauen KA, Bissell MJ, Korn WM. Disruption of 3D tissue integrity facilitates adenovirus infection by deregulating the coxsackievirus and adenovirus receptor. *Proc Natl Acad Sci U S A*. 2003;100(4):1943–1948.
21. Mi K, Feng Z, Liu Z, et al. Self-assembling peptide RADA16 nanofiber scaffold for a cancer cell three-dimensional culture. *Iran Polym J*. 2009;18(10):801–810.
22. Zhang S. Fabrication of novel biomaterials through molecular self-assembly. *Nat Biotechnol*. 2003;21(10):1171–1178.
23. Gelain F, Bottai D, Vescovi A, Zhang S. Designer self-assembling peptide nanofiber scaffolds for adult mouse neural stem cell 3-dimensional cultures. *PLoS One*. 2006;1:e119.
24. Ellis-Behnke RG, Liang YX, You SW, et al. Nano neuro knitting: peptide nanofiber scaffold for brain repair and axon regeneration with functional return of vision. *Proc Natl Acad Sci U S A*. 2006;103(13): 5054–5059.
25. Yu DG, Zhu LM, Branford-White CJ, et al. Solid dispersions in the form of electrospun core-sheath nanofibers. *Int J Nanomedicine*. 2011; 6:3271–3280.
26. Yu DG, Yu JH, Chen L, Williams GR, Wang X. Modified coaxial electrospinning for the preparation of high-quality ketoprofen-loaded cellulose acetate nanofibers. *Carbohydr Polym*. 2012;90(2): 1016–1023.
27. Yu DG, Zhou J, Chatterton NP, Li Y, Huang J, Wang X. Polyacrylonitrile nanofibers coated with silver nanoparticles using a modified coaxial electrospinning process. *Int J Nanomedicine*. 2012;7:5725–5732.
28. Velasco-Velázquez MA, Homsi N, De La Fuente M, Pestell RG. Breast cancer stem cells. *Int J Biochem Cell Biol*. 2012;44(4):573–577.
29. Ponti D, Costa A, Zaffaroni N, et al. Isolation and in vitro propagation of tumorigenic breast cancer cells with stem/progenitor cell properties. *Cancer Res*. 2005;65(13):5506–5511.

30. Ricardo S, Vieira AF, Gerhard R, et al. Breast cancer stem cell markers CD44, CD24 and ALDH1: expression distribution within intrinsic molecular subtype. *J Clin Pathol*. 2011;64(11):937–946.
31. Lee GY, Kenny PA, Lee EH, Bissell MJ. Three-dimensional culture models of normal and malignant breast epithelial cells. *Nat Methods*. 2007;4(4):359–365.
32. Weaver VM, Lelièvre S, Lakins JN, et al. Beta4 integrin-dependent formation of polarized three-dimensional architecture confers resistance to apoptosis in normal and malignant mammary epithelium. *Cancer Cell*. 2002;2(3):205–216.
33. Mi K, Wang G, Liu Z, Feng Z, Huang B, Zhao X. Influence of a self-assembling peptide, RADA16, compared with collagen I and Matrigel on the malignant phenotype of human breast-cancer cells in 3D cultures and in vivo. *Macromol Biosci*. 2009;9(5):437–443.
34. Ling PM, Cheung SW, Tay DK, Ellis-Behnke RG. Using self-assembled nanomaterials to inhibit the formation of metastatic cancer stem cell colonies in vitro. *Cell Transplant*. 2011;20(1):127–131.
35. Andarawewa KL, Erickson AC, Chou WS, et al. Ionizing radiation predisposes nonmalignant human mammary epithelial cells to undergo transforming growth factor beta induced epithelial to mesenchymal transition. *Cancer Res*. 2007;67(18):8662–8670.
36. Sheridan C, Kishimoto H, Fuchs RK, et al. $CD44^+/CD24^-$ breast cancer cells exhibit enhanced invasive properties: an early step necessary for metastasis. *Breast Cancer Res*. 2006;8(5):R59.
37. Li Q, Liu BC, Lv LL, Ma KL, Zhang XL, Phillips AO. Monocytes induce proximal tubular epithelial-mesenchymal transition through NF-kappa B dependent upregulation of ICAM-1. *J Cell Biochem*. 2011; 112(6):1585–1592.
38. Rothlein R, Dustin ML, Marlin SD, Springer TA. A human intercellular adhesion molecule (ICAM-1) distinct from LFA-1. *J Immunol*. 1986; 137:1270–1274.
39. Christgen M, Lehmann U. MDA-MB-435: the questionable use of a melanoma cell line as a model for human breast cancer is ongoing. *Cancer Biol Ther*. 2007;6(9):1355–1357.
40. Rae JM, Creighton CJ, Meck JM, Haddad BR, Johnson MD. MDA-MB-435 cells are derived from M14 melanoma cells – a loss for breast cancer, but a boon for melanoma research. *Breast Cancer Res Treat*. 2007;104(1):13–19.
41. Zhang Q, Fan H, Shen J, Hoffman RM, Xing HR. Human breast cancer cell lines co-express neuronal, epithelial, and melanocytic differentiation markers in vitro and in vivo. *PLoS One*. 2010;5(3):e9712.